Journal of Solid Mechanics Vol. 15, No. 4 (2023) pp. 369-382
DOI: 10.60664/jsm.2024.3031771

Research Paper

Thermal buckling analysis of temperature dependent porous FGM Mindlin nano circular plate on elastic foundation

M.M. Mohieddin Ghomshei *

Department of Mechanical Engineering, Karaj Branch, Islamic Azad University, Karaj, Alborz, 3149968111, Iran

Received 2 March 2023; accepted 5 August 2023

ABSTRACT

In the present work, the symmetric thermal buckling behavior of shear deformable heterogonous nano/micro circular porous plates resting on a two parameter foundation is studied. The material behavior of the nano plate is modeled by the modified couple stress theory. The plate material properties assumed to be graded across the thickness direction according to a simple power law, and have a uniform open void porosity. Using Mindlin's plate theory and the nonlinear von-Karman strain field and implementing the energy method, the plate stability equations together with the membrane equilibrium equation are derived and expressed in terms of the displacement field components. Then the nondimensionalized forms of the equations are derived using differential quadrature method (DQM). The resulting eigenvalue problem is solved to evaluate the plate critical buckling temperature difference. Convergence and comparative studies are carried out. Also the influences of some important parameters including length scale factor, porosity factor and Winkler& Pasternak stiffness coefficients are investigated.

Keywords: Thermal buckling; Circular nano/micro plate; FGM; Porous material; DQM.

1 INTRODUCTION

REGARDING the great stiffness and high temperature resistance, functionally graded materials (FGMs) are widely used specially in small scale structures. Nano/micro functionally graded plates are a new generation of advanced material systems which have found important applications in different engineering fields. Due to existence of nonlocal effects, classical continuum theories cannot accurately model the mechanical behavior of such small scale structures. So a number of size-dependent continuum mechanics models have been developed to take into account the small scale effects, such as the strain gradient theory (SGT) [1] and the modified couple stress theory (MCST) [2].

* Corresponding author. Tel.: +98 263 4259571-9.
E-mail address: mm.ghomshei@iau.ac.ir

In 2009 Duan and Wang [3] investigated the deformation of a single layer, circular, graphene sheet under a central point load by carrying out molecular mechanics (MM) simulations. The bending and stretching of the grapheme sheet are characterized by using the von Karman plate theory. It is shown that, with properly selected parameters, the von Karman plate theory can provide a remarkably accurate prediction of the graphene sheet behavior under linear and nonlinear bending and stretching. In 2010 Shen et al. [4] presented nonlinear vibration behavior analysis for a simply supported, rectangular, single layer graphene sheet in thermal environments. The single layer graphene sheet is modeled as a nonlocal orthotropic plate which contains small scale effects. The nonlinear vibration analysis is based on thin plate theory with a von Kármán-type of kinematic nonlinearity. The thermal effects are also included and the material properties are assumed to be temperature-dependent and are obtained from molecular dynamics simulations. In 2013 Jabbarzadeh et al. [5] studied nonlinear bending behavior of single-layered circular graphene sheet using nonlocal continuum mechanics and plate first order shear deformation theory (FSDT). Differential quadrature method is used to discretize the equilibrium equations. The effect of nonlocal parameter, number of grid points, etc. are investigated on the deflection of graphene sheet. In 2013, Wang et al [6] proposed a nonclassical mathematical model and an algorithm for the axisymmetrically nonlinear free vibration analysis of a circular microplate, based on the modified couple stress theory and von Kármán geometrically nonlinear theory. The numerical results indicate that the microplates modeled by the modified couple stress theory cause more stiffness than modeled by the classical continuum plate theory. In 2014 Ghiasian et al. [7] presented an exact solution for the bifurcation behavior of moderately thick heated annular plates made of FGMs based on FSDT. Properties of the graded plate are distributed across the thickness based on the simple power law form. Temperature-dependency of the material properties is also taken into account. It is shown that the fundamental buckled configuration of annular plates may be asymmetric. Jabbari et al. [8] in 2014 presented the buckling analysis of thermal loaded solid circular plate made of porous material. The equations are based on the Sanders non-linear strain-displacement relation. Using their mathematical model, they studied the effect of pores distribution and thermal distribution on the critical buckling temperature. Ansari et al. [9] in 2015 studied bending, buckling and free vibration analysis of size-dependent functionally graded circular/annular microplates based on the modified strain gradient elasticity theory. The size effects are captured through using three higher-order material constants. They applied Hamilton's principle together with linear strain field to derive the governing differential equations. the generalized differential quadrature (GDQ) method is employed to discretize the governing equations. Eshraghi et al [10] in 2016 introduced solution methods capable of treating static bending and free vibration problems involving thermally loaded functionally graded annular and circular micro-plates. Formulation is based on modified couple stress theory. Shojaeefard et al. [11] in 2017 numerically studied the free vibration and thermal buckling of micro temperature dependent FG porous circular plate subjected to a nonlinear thermal load, using both classical and the first-order shear deformation theories in conjunction with the modified couple stress theory. Effect of FG power index, size dependency, temperature-change, geometrical dimensions as well as some other parameters are presented in this work. In 2017 Lin et al. [12] investigates the scale effect on nonlinear behavior of a clamped–clamped circular graphene sheet nanoplate actuator, which is electrostatically actuated by various van der Waals (vdW) forces, tensile loads, and hydrostatic pressures. The circular nanoplate model is developed by using Eringen's nonlocal elasticity theory. In 2019 Farzam and Hassani [13] investigates the static bending and buckling behaviors of functionally graded microplates under mechanical and thermal loads by using isogeometric analysis (IGA) and modified strain gradient theory (MSGT). The material properties are assumed to be temperature-dependent. They showed that the type of functionally graded material is an important parameter for thermal analysis. In 2020 Ghobadi et al. [14] investigated the effects of flexoelectricity on thermo-electro-mechanical behavior of a functionally graded electro-piezo-flexoelectric nano-plate using flexoelectric modified and the Kirchhoff classic theories and energy method. The nano-plate behavior is analyzed under mechanical, electrical, and thermal loadings with different boundary conditions. In 2021 Ahmad Pour et al. [15] analyzed the thermal buckling of circular bilayer Graphene sheets resting on an elastic matrix based on nonlocal differential constitutive relation of Eringen and FSDT. The effects of the small scale parameter, vdW forces, aspect ratio, elastic foundation, and boundary conditions are considered in detail. In 2021 Rajabi et al. [16] analyze a nanoplate with a central crack under distributed transverse load based on modified nonlocal elasticity theory. It was shown that the complete modified nonlocal elasticity theory does not show any singularity at the crack-tip unlike the classical theory; therefore, the method presented is a suitable method for analysis of the nanoplates with a central crack. Kiarasi et al. [17] in 2021 studied the buckling behavior of functionally graded (FG) porous rectangular plates subjected to different loading conditions. Three different porosity distributions are assumed throughout the thickness, namely, a nonlinear symmetric, a nonlinear asymmetric and a uniform distribution. A novel approach is proposed here based on a combination of the generalized differential quadrature (GDQ) method and finite elements (FEs), labeled here as the FE-GDQ method. Saini et al. [18] in 2022 investigated the size-dependent thermal buckling analysis of nonuniform

functionally graded asymmetric circular and annular nanodiscs, on the basis of Kirchhoff's plate theory, Eringen's nonlocal elasticity theory, and physical neutral plane. The thickness of the nanodiscs is assumed to be varying linearly and parabolically in the radial direction. The size-dependent stability equation is obtained from Euler-Lagrange's equation which is derived from Hamilton's principle. This equation and corresponding boundary conditions are discretized by the differential quadrature method (DQM) and provide an eigenvalue problem. The numerical value of the lowest eigenvalue is reported as a critical temperature difference on the surfaces of the nanodiscs.

The small-scale effects on circular open void porous .nano/micro circular plates in thermal environment have not been understood fully in the literature. In the present research work the thermal buckling behavior of nano/micro porous circular plates on a winkler-Pasternak foundation are investigated in detail. The temperature dependency is considered for the material properties, with a uniform open void porosity in the plate. For the constitutive behavior the modified couple stress theory is implemented. FSDT plate theory, von-Karman strain field with the energy method is employed to derive equilibrium equations. The adjacent equilibrium method is applied to derive the set of stability equations. At last differential quadrature method has been used to solve the set of stability equations numerically. In Ref. [11] as more similar work to the present research work, it should be noted that in this reference linear strain field has been implemented, also the plate is not placed on a foundation, and moreover nondimensionalizing is not applied to the formulation and results. The novelty of the present work in comparison to the previous published works can be at first considering a Winkler-Pasternak foundation for the temperature dependent nano/micro porous circular plates. Next, implementing modified couple stress theory with nonlinear von-Karman strain field for investigating the buckling problem, and the third is non-dimensionalizing the equations so that the formulation and results take a generality.

2 MATHEMATICAL FORMULATION

2.1 The Geometric Parameters and Material Properties

A FGM nano circular porous plate of radius b and thickness h resting on a two parameter foundation is under investigation as shown in Fig. 1. The radial coordinate is denoted by r and the transverse coordinate is denoted by z with its origin located on the plate mid-surface. The metal volume fraction, V_m, assumed to vary according to a simple power law along the thickness coordinate axis z, while has symmetry with respect to the plate mid-surface, which can be stated as

$$V_m = \left(1 - \frac{2|z|}{h}\right)^n, \qquad \text{for} \quad -\frac{h}{2} \le z \le \frac{h}{2} \tag{1}$$

where n is termed as the volume fraction index, with $n = 0$, $n = \infty$ representing two extreme cases of pure metal and pure ceramic plates respectively. The ceramic volume fraction, V_c, can simply be determined by

$$V_c = 1 - V_m \tag{2}$$

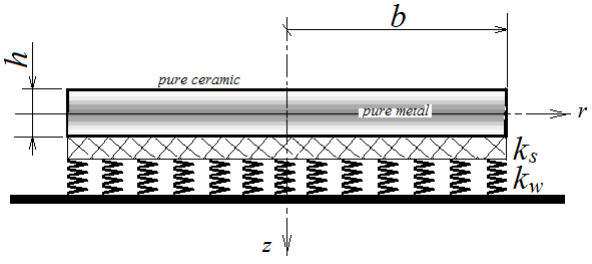

Fig.1
Geometric and foundation parameters of FG nano circular porous FGM plate.

The FGM properties such as Young modulus, E, and the coefficient of thermal expansion, α, can be determined by the rule of mixture, while Poisson's ratio, ν, is assumed to remain constant across the thickness, thus

$$E=V_mE_m+V_cE_c, \qquad \alpha=V_m\alpha_m+V_c\alpha_c, \qquad \nu=\nu_m=\nu_c \tag{3}$$

where E_m,α_m,ν_m are respectively Young modulus, thermal expansion coefficient and Poisson's ratio of metal, while E_c,α_c,ν_c are those of ceramic.

For the constitutive behavior of the nano-plate the modified couple stress theory is adopted as below [11]:

$$\begin{aligned}&\sigma_{ij}=2\mu\left(\varepsilon_{ij}-\alpha\Delta T\delta_{ij}\right)+\lambda\delta_{ij}\left(\varepsilon_{kk}-3\alpha\Delta T\right),\\&m_{ij}=2\mu l^2\,\chi_{ij}\end{aligned} \tag{4}$$

where σ_{ij} Cauchy's stresses, ε_{ij} strains, λ and μ are Lame's constants. Also α, ΔT, δ_{ij} are respectively coefficient of thermal expansion, temperature difference and Kroneker delta. Furthermore, χ_{ij} is the curvature change tensor, that is same as κ_{ij} in this work. Also m_{ij} is the tensor of modified couple. Lame's constants in terms of the poison's ratio ν and elastic modulus E are to be written as:

$$\lambda=\frac{\nu E}{(1+\nu)(1-2\nu)}, \qquad \mu=\frac{E}{2(1+\nu)}=G \tag{5}$$

in that, considering the porosity factor , E, ν and α can be written as [19]:

$$E=(1-\beta)^2E_0, \qquad \nu=\nu_0, \qquad \alpha=\alpha_0 \tag{6}$$

Where, E_0, ν_0 and α_0 are the elastic modulus, poison's ratio and coefficient of thermal expansion of a material without porosity.

The temperature dependence of the components, metal and ceramic, is stated by [13]:

$$P(T)=P_0\left(P_{-1}T^{-1}+1+P_1T^1+P_2T^2+P_3T^3\right) \tag{7}$$

The coefficients of temperature in the above equation are tabulated in Table 1. The reference temperature T_0 is assumed equal to 300 K.

2.2 Kinematic and Constitutive Relations

Regarding the moderately thick plate assumption, the FSDT is used herein to estimate the displacement field within the circular plate. Based on the theory the axisymmetric displacement components are stated as

$$u(r,z)=u_0(r)+z\varphi(r), \qquad w(r,z)=w(r) \tag{8}$$

in that u, w are the radial and lateral displacements respectively, and φ is the total rotation about the circumferential axis. Also, u_0 denotes the radial displacement at mid-plane. In polar coordinates the strain components are written as [20]

$$\varepsilon_r=\varepsilon_r^0+\kappa_rz, \qquad \varepsilon_\theta=\varepsilon_\theta^0+\kappa_\theta z, \qquad \gamma_{rz}=\varphi+w_{,r} \tag{9}$$

where, based on the von-Karman assumption suitable for moderately large class of deflections, the mid-plane strains $\varepsilon_r^0,\varepsilon_\theta^0$, and curvatures κ_r,κ_θ are given in terms of displacement components as [20]

$$\varepsilon_r^0=u_{0,r}+\frac{1}{2}(w_{,r})^2, \qquad \varepsilon_\theta^0=\frac{u_0}{r}, \qquad \kappa_r=\varphi_{,r}, \qquad \kappa_\theta=\frac{\varphi}{r} \tag{10}$$

Here, the differentiation with respect to r is denoted by $(\,)_{,r}$.

Assuming a material linear behavior during the whole pre-buckling and buckling deformations, and by using the first of Eqs. (4), the stress-strain relationships for the FG plate may be expressed as

$$\begin{aligned}&\sigma_r=\frac{E}{1-\nu^2}(\varepsilon_r+\nu\varepsilon_\theta)-\frac{E\alpha}{1-\nu}\Delta T,\\&\sigma_\theta=\frac{E}{1-\nu^2}(\varepsilon_\theta+\nu\varepsilon_r)-\frac{E\alpha}{1-\nu}\Delta T, \qquad \tau_{rz}=\frac{E}{2(1+\nu)}\gamma_{rz}\end{aligned} \tag{11}$$

in that $\sigma_r,\sigma_\theta,\tau_{rz}$ are the stress components. Substituting from Eq. (9), into Eq. (11), then integrating the resulting expressions over the thickness, yields the following equality for non-zero force / moment resultants

$$\begin{Bmatrix} N_r \\ N_\theta \\ M_r \\ M_\theta \\ Q_r \end{Bmatrix} = \begin{bmatrix} A_{11} & A_{12} & 0 & 0 & 0 \\ A_{12} & A_{22} & 0 & 0 & 0 \\ 0 & 0 & D_{11} & D_{12} & 0 \\ 0 & 0 & D_{12} & D_{22} & 0 \\ 0 & 0 & 0 & 0 & A_{55} \end{bmatrix} \begin{Bmatrix} \varepsilon_r^0 \\ \varepsilon_\theta^0 \\ \kappa_r \\ \kappa_\theta \\ \gamma_{rz}^0 \end{Bmatrix} - \begin{Bmatrix} N_r^T \\ N_\theta^T \\ M_r^T \\ M_\theta^T \\ 0 \end{Bmatrix} \tag{12}$$

where A_{ij}'s, and D_{ij}'s are respectively the components of extensional and bending stiffness, defined by

$$A_{11} = A_{22} = A = \frac{E_1}{1-\nu^2},\ A_{12} = \frac{\nu E_1}{1-\nu^2} = \nu A_{11},$$
$$A_{55} = \frac{K(1-\nu)}{2} A_{11},\ D_{11} = D_{22} = \frac{E_3}{1-\nu^2},\ D_{12} = \nu D_{11} \tag{13}$$

where $K = \pi^2/12$ denotes the transverse shear correction factor, and $(E_1, E_3) = 2\int_0^{h/2} (1, z^2) E(z)\, dz$ which can be evaluated, by substituting in that from Eqs.(2,3) and Eq.(6) for $E(z)$, as

$$E_1 = (1-\beta)^2 \left(E_c - \frac{E_{cm}}{n+1} \right) h,$$
$$E_3 = (1-\beta)^2 \left(E_c - \frac{6E_{cm}}{(n+1)(n+2)(n+3)} \right) \frac{h^3}{12} \tag{14}$$

where E_c, E_m are elastic moduli of ceramic and metal without porosity and $E_{cm}=E_c-E_m$. Also in Eq. (12), N_r^T, N_θ^T are the thermal membrane forces and M_r^T, M_θ^T are the thermal moments which are given by

$$N_r^T = \int_{-h/2}^{h/2} \sigma_r^T dz = \frac{(1-\beta)^2}{1-\nu} \left(E_c \alpha_c - \frac{E_c \alpha_{cm} + E_{cm} \alpha_c}{n+1} + \frac{E_{cm} \alpha_{cm}}{2n+1} \right) \Delta T h,$$
$$M_r^T = 0, \qquad (N_\theta^T, M_\theta^T) = (N_r^T, M_r^T) \tag{15}$$

where $\alpha_{cm} = \alpha_c - \alpha_m$.

Moreover, the integrals of modified couples over plate thickness Ω_r, Ω_θ are defined as:

$$\Omega_r = \int m_r dz = \Gamma \varphi_{,r}\ , \qquad \Omega_\theta = \int m_\theta dz = \Gamma \frac{\varphi}{r} \tag{16}$$

in that

$$\Gamma = \left(E_c l_c^{\,2} - \frac{E_{cm} l_c^{\,2}}{n+1} + \frac{E_c l_{cm}^{\,2}}{2n+1} - \frac{E_{cm} l_{cm}^{\,2}}{3n+1} - \frac{2E_c l_c l_{cm}}{n+1} + \frac{2E_{cm} l_c l_{cm}}{2n+1} \right) \frac{(1-\beta^2)h}{1+\nu} \tag{17}$$

2.3 Equilibrium and Stability Equations

The plate equilibrium equations may be derived by employing the energy method as

$$\delta (U_C + U_{NC} - W) = 0 \tag{18}$$

Where U_C, U_{NC} and W are respectively classical strain energy, non-classical strain energy and the external thermal work, that are calculated by:

$$U_C = \frac{1}{2} \int_{R_i}^{R_o} \left(N_r \varepsilon_r^0 + N_\theta \varepsilon_\theta^0 + Q \gamma_{rz}^0 + M_r \kappa_r + M_\theta \kappa_\theta \right) 2\pi r\, dr,$$
$$U_{NC} = \frac{1}{2} \int_{R_i}^{R_o} \left(\Omega_r \kappa_r + \Omega_\theta \kappa_\theta \right) 2\pi r\, dr, \tag{19}$$
$$W = -\frac{1}{2} \int_A N_r^T \left(\frac{\partial w}{\partial r} \right)^2 dA - \frac{1}{2} \int_A w \left[k_w w - k_s \left(\frac{\partial^2 w}{\partial r^2} + \frac{1}{r} \frac{\partial w}{\partial r} \right) \right] dA$$

Now, substituting from Eq. (19) into Eq. (18), then implementing the essential variational lemma, the equilibrium equations of nano circular plate on a Winkler/Pasternak foundation are derived as follows:

$$\begin{aligned}
&\delta u: \quad \frac{d}{dr}\left[Ar\left(u_{,r}+\frac{1}{2}w_{,r}^2+\nu\frac{u}{r}-\frac{N_r^T}{2A}\right)\right]-A\left(\nu u_{,r}+\frac{\nu}{2}w_{,r}^2+\frac{u}{r}-\frac{N_r^T}{2A}\right)=0,\\
&\delta w: \quad \frac{d}{dr}\left\{r\left[Aw_{,r}\left(u_{,r}+\frac{1}{2}w_{,r}^2+\nu\frac{u}{r}+\frac{N_r^T}{2A}\right)+\frac{AK(1-\nu)}{2}(\varphi+w_{,r})\right]\right\}=k_w rw-k_s\left(rw_{,rr}+w_{,r}\right),\\
&\delta\varphi: \quad \frac{d}{dr}\left[(D+\Gamma)r\varphi_{,r}\right]-\frac{AK(1-\nu)}{2}r\left(\varphi+w_{,r}\right)-\left[\nu D\varphi_{,r}+\left(D+\nu D+\Gamma\right)\frac{\varphi}{r}\right]=0
\end{aligned} \tag{20}$$

where k_w , k_s are respectively the Winkler's coefficient and Pasternak's coefficient of the elastic foundation. It is assumed that the foundation acts in compression as well as in tension. Implementing the adjacent equilibrium method [21] on the equilibrium equations expressed in terms of displacement components, the linearized stability equations of the plate associated with the onset of buckling are derived as follows

$$\begin{aligned}
&\frac{d}{dr}\left[Ar\left(u_{,r}^1+w_{,r}^0w_{,r}^1+\nu\frac{u^1}{r}\right)\right]-A\left(\nu u_{,r}^1+\nu w_{,r}^0w_{,r}^1+\frac{u^1}{r}\right)=0,\\
&\frac{d}{dr}\left[Arw_{,r}^0\left(u_{,r}^1+w_{,r}^0w_{,r}^1+\nu\frac{u^1}{r}\right)\right]-Arw_{,r}^1\left(u_{,r}^0+\frac{1}{2}w_{,r}^{02}+\nu\frac{u^0}{r}+\frac{N_r^T}{2A}\right)-\frac{AK(1-\nu)}{2}(\varphi^1+w_{,r}^1)=\\
&\qquad k_w rw^1-k_s\left(rw_{,rr}^1+w_{,r}^1\right),\\
&\frac{d}{dr}\left[(D+\Gamma)r\varphi_{,r}^1\right]-\frac{AK(1-\nu)}{2}r\left(\varphi^1+w_{,r}^1\right)-\nu D\varphi_{,r}^1-\left(D+\nu D+\Gamma\right)\frac{\varphi^1}{r}=0
\end{aligned} \tag{21}$$

where u^0, w^0, φ^0 designate the prebuckling state at the onset of buckling, and u^1, w^1, φ^1 are the increments of the displacement components of an adjacent equilibrium state with respect to the prebuckling state. Note that for the problem under investigation, there are no lateral loading and thermal moments ($p=M_r^T=0$), therefore $w^0=\varphi^0=0$, and the membrane prebuckling displacement u^0 may be obtained by solving the first of the equilibrium equations, which may be stated as

$$r^2Au_{,rr}^0+(r^2A_{,r}+rA)u_{,r}^0+(\nu rA_{,r}-A)u^0=r^2N_{r,r}^T \tag{22}$$

Here, i.e. for the case of uniform plate, $A_{,r}$=$A_{11,r}$=0. For generality, it is more appropriate to express the equilibrium and stability equations in dimensionless form. The following dimensionless quantities are defined and used hereafter in this work.

$$\begin{aligned}
&\xi=\frac{r}{b},\ \ \bar{u}_0=\frac{u_0}{b},\ \ \bar{w}=\frac{w}{b},\ \ \bar{u}^1=\frac{u_0^1}{b},\ \ \bar{w}^1=\frac{w^1}{b},\ \ \mu=\frac{2}{1-\nu},\\
&\bar{k}_w=\frac{k_wb^2}{A_{55}},\quad \bar{k}_s=\frac{k_s}{A_{55}},\quad \bar{N}_r^T=\frac{N_r^T}{A_{55}},\quad \bar{N}_r^{T\prime}=\frac{bN_{r,r}^T}{A_{55}},\quad \bar{\Gamma}=\frac{\Gamma}{D},\quad \bar{\Gamma}'=\frac{b\Gamma_{,r}}{D},\quad \bar{F}=\frac{b^2A_{55}}{D_{11}}
\end{aligned} \tag{23}$$

Using the dimensionless quantities and after performing some algebraic operations, the dimensionless forms of Eq. (22), and the last two stability equations of Eq. (21), are derived respectively as

$$f_1u_{,rr}^0+f_2u_{,r}^0+f_3u^0=f_4 \tag{24}$$

and

$$\begin{aligned}
&f_5\,\bar{w}_{,\xi}^1+f_6\,\varphi_{,\xi\xi}^1+f_7\,\varphi_{,\xi}^1+f_8\varphi^1=0,\\
&f_9\bar{w}_{,\xi\xi}^1+f_{10}\bar{w}_{,\xi}^1+f_{11}\bar{w}^1+f_{12}\varphi_{,\xi}^1+f_{13}\varphi^1=0
\end{aligned} \tag{25}$$

In Eqs .(24, 25) the coefficients f_i's are defined by

$$f_1=\xi^2,\quad f_2=\xi,\quad f_3=-1,\quad f_4=\frac{K}{\mu}\xi^2\bar{N}_r^{T\prime},$$
$$f_5=-\bar{F}\xi^2,\quad f_6=\xi^2\left(1+\bar{\Gamma}\right),\quad f_7=\xi^2\bar{\Gamma}'+\xi\left(1+\bar{\Gamma}\right),$$
$$f_8=-\left(\bar{F}\xi^2+1+\bar{\Gamma}\right),\quad f_9=\xi+\frac{\mu}{K}\xi+\nu\frac{\mu}{K}\bar{u}+\xi\bar{k}_s-\xi\bar{N}_r^T,$$
$$f_{10}=\frac{\mu}{K}\xi\bar{u}_{,\xi\xi}+\frac{\mu}{K}\left(1+\nu\right)\bar{u}_{,\xi}+1+\bar{k}_s-\bar{N}_r^T--\xi\bar{N}_r^{T\prime} \tag{26}$$
$$,\quad f_{11}=-\bar{k}_w\xi,\quad f_{12}=\xi,\quad f_{13}=1$$

Also, the nondimensionalized forms of the boundary conditions corresponding to Eq.(24) and Eq.(25) become

$$\text{At } \xi=0:\ \bar{u}^0=0,\quad \text{At } \xi=1:\ \bar{u}^0=0 \tag{27}$$

and

$$\text{At } \xi=0:\ \bar{u}^1=0,\ d\bar{w}^1/d\xi=0,\ \varphi^1=0,$$
$$\text{At } \xi=1:\ \bar{u}^1=0,\ \bar{w}^1=0,\ \varphi^1=0\ (\text{for clamped edge})\ or\ \bar{u}^1=0,\ \bar{w}^1=0,\ \varphi^1_{,\xi}+\nu\varphi^1=0\ (\text{for simple edge}) \tag{28}$$

3 NUMERICAL SOLUTION PROCEDURE

In this work a numerical solution scheme based on the differential quadrature method is implemented for discretizing the governing set of ordinary differential equations (ODEs) of variable coefficients, in that the weighting coefficients are determined by the procedure introduced by Shu and Richards. To ensure the convergence of DQ approximation, an unequally spaced grid point distribution so-called Chebyshev nodes is utilized. Applying the differential quadrature rule to the equilibrium equation, Eq. (24) and stability equations, Eqs. (25), the discretized forms of the equations are derived respectively as

$$f_{1i}\sum_{j=1}^{N}C_{ij}^{(2)}U_j^0+f_{2i}\sum_{j=1}^{N}C_{ij}^{(1)}U_j^0+f_{3i}U_i^0=f_{4i},\qquad i=1,2,\ldots,N \tag{29}$$

And

$$f_{5i}\sum_{j=1}^{N}C_{ij}^{(1)}W_j+f_{6i}\sum_{j=1}^{N}C_{ij}^{(2)}\Phi_j+f_{7i}\sum_{j=1}^{N}C_{ij}^{(1)}\Phi_j+f_{8i}\Phi_i=0,$$
$$f_{9i}\sum_{j=1}^{N}C_{ij}^{(2)}W_j+f_{10i}\sum_{j=1}^{N}C_{ij}^{(1)}W_j+f_{11i}W_i \tag{30}$$
$$+f_{12i}\sum_{j=1}^{N}C_{ij}^{(1)}\Phi_j+f_{13i}\Phi_i=0,\qquad i=1,2,\ldots,N$$

where N is the selected number of grid points, $C_{ij}^{(1)}$, $C_{ii}^{(2)}$ are the weighting coefficients of the first and second order derivatives respectively, and

$$f_{ki}=f_k(\xi_i),\qquad k=1,2,\ldots,13,$$
$$U_i^0=\bar{u}^0(\xi_i),\qquad U_i=\bar{u}^1(\xi_i), \tag{31}$$
$$W_i=\bar{w}^1(\xi_i),\qquad \Phi_i=\varphi^1(\xi_i),\qquad i=1,2,\ldots,N$$

It should be noted that because in some of the f_k's the displacement response u are arisen, an iterative loop is applied in the MATLAB program. Moreover, to apply the temperature dependency, the f_k's become temperature dependent functions. Therefore another iterative loop is implemented in the computer code.

The discretized forms of the boundary conditions given by Eq. (27) and Eq. (28) are respectively written as

$$U_1^0=0,\qquad U_N^0=0 \tag{32}$$

and

$$\begin{aligned} &U_1 = 0, \quad \Phi_1 = 0, \quad \sum_{j=1}^{N} C_{1j}^{(1)} W_j = 0, \quad \text{(center point)} \\ &U_N = 0, \quad W_N = 0, \quad \Phi_N = 0, \quad \text{(clamped edge)} \\ &U_N = 0, \quad W_N = 0, \quad \sum_{j=1}^{N} C_{Nj}^{(1)} \Phi_j + \nu \Phi_N = 0, \quad (S.S.\ \text{edge}) \end{aligned} \tag{33}$$

At first, the discretized form of the prebuckling equilibrium equation, Eqs. (29), with corresponding B.C's. which constitute a set of N linear algebraic equations, are solved simultaneously to find the prebuckling radial displacements, U_{0i}'s, as multipliers of the temperature difference ΔT . Note that the right-hand side of Eqs. (29), f_{4i}'s, are linear expressions of ΔT . Then, substituting from Eq.(15) for N_r^T and the expressions found for the prebuckling radial displacements U_i^0's into Eqs.(30), and after imposition of the boundary conditions, Eqs.(33), a set of $3N$ linear homogenous equations in terms of W_i's and Φ_i's are obtained. Implementing the nontrivial solution condition on the set of equations, leads to an algebraic equation in terms of ΔT , which its smallest positive real root is the critical buckling temperature difference, ΔT_{cr} . The operations are done in the two abovementioned iterative loops until the convergence criteria are satisfied.

4 NUMERICAL RESULTS AND DISCUSSION

Numerical results are extracted for FGM porous plates made of a mixture of SUS304 as metal and Si3N4 as ceramic, with coefficients of temperature dependent material properties as listed in Table 1, unless otherwise specified. Before conducting the comparative and parametric studies, the convergence of the present DQM is evaluated by investigating the effect of the selected number of grid points on the normalized error arisen in the computed value of the plate buckling temperature.

Table 1
Coefficients of temperature dependent material properties [13].

Material	P_0	P_{-1}	$P_1\times10^{-4}$	$P_2\times10^{-7}$	$P_3\times10^{-11}$
Si3N4 (Ceramic)					
E (Pa)	348.43×10^{9}	0	-3.070	2.160	-8.946
α (1/K)	5.8723×10^{-6}	0	9.095	0	0
ν	0.2400	0	0	0	0
SUS304 (Metal)					
E (Pa)	201.04×10^{9}	0	3.079	-6.534	0
α (1/K)	12.330×10^{-6}	0	8.086	0	0
ν	0.3262	0	-2.002	3.797	0

4.1 Convergence Study

The convergence of the presented DQ scheme is studied for a nano circular plate. Seven different node numbers N=5, 7, 9, 11, 13, 15, 17considered, and convergence studied for three clamped plate of h/l=1/50, 1/40, 1/30 for the case of Temperature dependent (TD) material properties, and the results are as depicted in Fig. 2. As can be seen in this figure, the convergence is fast, so that just by 11 nodes the normalized percentage error become 0.0004% , and by considering 13 nodes the error percent ceases to 0.0001%. The results that are presented here is extracted by considering 15 nod points.

4.2 Validation

Comparative studies are carried out in two examples to validate the DQ formulation. As the first example, the values of the critical temperature change ΔTcr for nonporous macro-scale circular clamped homogeneous plates subjected to uniform thermal loading without elastic foundation of six different aspect ratios (h/b) are computed by the present DQM, and the results are listed in Table 2 along with those reported in Ref. [7]. The results are presented for both cases of temperature independent (TID) and temperature dependent (TD) properties. The porosity factor set to zero. A good correspondence can be observed between the present results with those reported in the reference, so that for the case TID maximum normalized error percent is 1.0%, and for the case TD the maximum percentage normalized error is 1.34% . As the second verification, a comparison between the present DQM results for ΔTcr with those reported by Ref. [8] for solid circular clamped poro/ monotonus distribution plates subjected to uniform thermal loading without foundation is performed. In Table 3 the results for ΔTcr are presented for thin plates of 20 different aspect ratios (h/b), with the porosity β= 0.452277. The Table shows satisfactorily good correspondence, such that the average normalized error percent is less than 1%.

Table 2
A comparison between the results of the present work with those reported in Ref. [7] on ΔTcr (C) for solid circular clamped homogeneous plates subjected to uniform thermal loading.

			h/b					
			0.01	0.02	0.03	0.04	0.05	0.06
k=0	Present	TID	12.721	50.879	114.458	203.432	317.761	457.398
	Ref. [7]	TID	12.591	50.360	113.293	201.369	314.556	452.816
	Present	TD	12.593	48.942	105.464	177.854	262.179	355.314
	Ref. [7]	TD	12.480	48.667	105.361	178.581	264.548	360.140
k= ∞	Present	TID	6.219	24.873	55.954	99.449	155.340	223.603
	Ref. [7]	TID	6.245	24.979	56.194	99.879	156.020	224.596
	Present	TD	6.195	24.507	54.166	94.058	142.895	199.375
	Ref. [7]	TD	6.219	24.583	54.267	94.095	142.734	198.866

Table 3
A comparison between the results of the present work with those reported in Ref. [6 8] on ΔTcr (C) for solid circular clamped poro/monotonus distribution plates subjected to uniform thermal loading.

	h/b									
	.0021	.0040	.0057	.0076	.0094	0.011	.0125	.0139	.0152	.0166
Ref. [8]	266	788	1567	2860	4282	5831	7508	9185	11119	13053
Present	248	767	1550	2755	4215	5668	7455	9218	11023	13147
	h/b									
	.0191	.0204	.0216	.0226	.0238	.0248	.0259	.0269	.0279	.0289
Ref. [8]	17305	19753	22072	24518	26837	29412	31859	34562	37008	39841
Present	17404	19854	22258	24474	27022	29340	32000	34518	37131	39835

4.3 Parametric Survey

Parametric studies are conducted to investigate the influence of a number of parameters on the plate critical temperature change ΔTcr. Fig. 3 shows the variations of ΔTcr of nano plate without foundation with respect to the length scale ratio l/h, for the two case of TD amd TID for both clamped (CC) and simply supported (SS) edge conditions. It is observed that, ΔTcr has an inclining behavior with increasing length scale ratio l/h. This is because as the length scale ratio gets larger values, the small scale effects decreases and the plate approaches to macro scale plate without nonlocal effects, and therefore the critical temperature difference ΔTcr increases. Moreover the values of the TD case are considerably smaller than that of the case TID, because the temperature effect causes to material become softer, and consequently the critical temperature difference for thermal buckling decreases. Also

ΔTcr in CC edge condition are much larger than those of the SS. This is due to clamped edge is much harder than the simple edge conditions.

The effect of the porosity factor β on the variations of ΔT_{cr} with a length scale factor *l/h* of nano plate without foundation, has been depicted in Fig. 4 for the two case of TD and TID for both CC and SS edge conditions. It is observed that, ΔT_{cr} has a declining manner with the porosity factor β. This may be justified by the fact that since the uniform distribution porosity is considered in the plate, at the outer layers which have more ceramic with greater young modulus, the porosity ratio is same as that of the neutral surface. Therefore the bending stiffness's of the plate become weaker and thermal buckling take place at smaller temperature change. It should be noted that the porosity which considered in this work is of kind open void porosity. Moreover the values of the TD case is considerably smaller than those of the case TID as justified in the previous paragraph. Also values of ΔT_{cr} in CC edge condition are much larger than those of the SS condition. The justification also is as mentioned in the previous paragraph.

Fig. 5 shows the effect of the volume fraction index *n* on the variations of ΔT_{cr} with length scale factor *l/h* of FGM nano plate without foundation, for case TD, with CC edge. It is observed that, ΔT_{cr} increases as the volume fraction index *n* gets larger values. This can be explain in this way that as *n* gets larger values the percentage of ceramic in the plate symmetrically increases. As E_c is larger than E_m the critical temperature rise increases. Moreover as *n* gets larger values its influence becomes lesser so that as *n* approaches to infinity the influence ceases to zero. Also, as mentioned previously, ΔT_{cr} has an inclining manner as *l/h* gets larger values which is justified previously.

The effect of dimensionless Winkler stiffness coefficient $\bar{k}_w$ on the variation of ΔT_{cr} with length scale factor *l/h* of nano plate of CC edge conditions for TD case is presented in Fig. 6. It is observed that, ΔT_{cr} increases greatly as $\bar{k}_w$ gets larger values. However its influence becomes smaller for greater values of $\bar{k}_w$. Fig. 7 depicts the effect of dimensionless Pasternak stiffness coefficient $\bar{k}_s$ on the variation of ΔT_{cr} with length scale factor *l/h* of nano plate of CC edge conditions. Again it is observed that, ΔT_{cr} increases greatly as $\bar{k}_s$ gets larger values. But its influence becomes smaller for greater values of $\bar{k}_s$. This can be justified by noting the fact that as $\bar{k}_w$ or $\bar{k}_s$ gets larger values, the strain energy required to store in the system to buckle the plate increases. Therefore the critical buckling temperature increases as $\bar{k}_w$ or $\bar{k}_s$ increases.

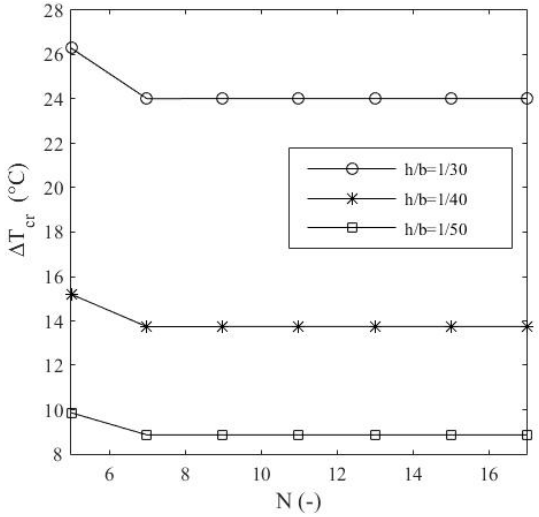

Fig.2

Convergence study of the DQM numerical model. Seven different node numbers N=5, 7, 9, 11, 13, 15, 17 considered, and convergence studied for three clamped plate of h/b=1/50, 1/40, 1/30 for case of TD.

5 CONCLUDING REMARKS

A numerical solution formulation based on the DQM is developed for axisymmetric thermal buckling analysis of uniform thickness FGM moderately thick circular nano/micro plates with uniform porosity resting on Winkler/Pasternak foundation, based on FSDT, von-Karman strain field and the modified couple stress theory, for both temperature dependent (TD) and temperature independent (TID) conditions. The convergence, validation and high accuracy of the proposed DQ formulation are investigated.

Parametric studies are conducted to investigate the influence of some important parameters on the buckling temperature. It is observed that ΔT_{cr} has a considerable inclining behavior with increasing length scale ratio *l/h*. For the case of uniformly distributed porosity, ΔT_{cr} has a declining manner with increasing the porosity factor β. ΔT_{cr} increases as the volume fraction index *n* gets larger values. Also it is observed that, ΔT_{cr} increases greatly as each one of $\overline{k}_w$ and $\overline{k}_s$ get larger values. However their influence become smaller for greater values of $\overline{k}_w$ or $\overline{k}_s$. The influence of temperature dependency on the values of ΔT_{cr} is investigated. The values corresponding to the TD case is considerably smaller than those of the case TID. Also, the effect of the plate edge condition on the values of ΔT_{cr} is studied. The values corresponding to the CC case is considerably larger than those of the case SS edge condition.

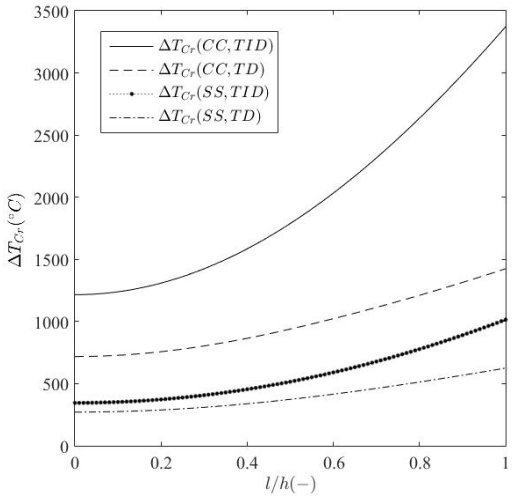

Fig.3
Effect of *l/h* on *ΔTcr* for two case of TD and TID for both CC and SS edge conditions. (*β*=0.5*,* *n*=1, *h/b*=0.1).

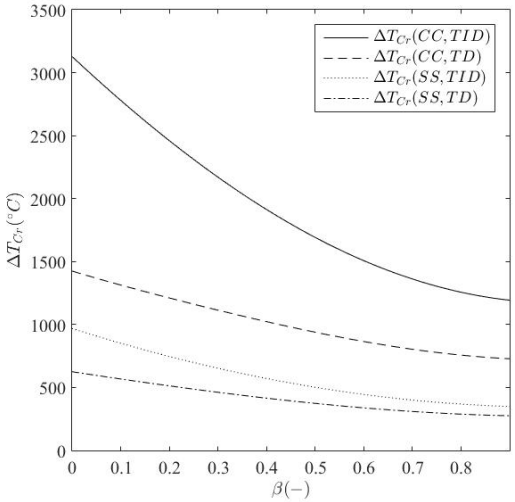

Fig.4
Effect of porosity factor *β* on the variation of ΔT_{cr} with *l/h* of nano plate without foundation for two cases of TD and TID for both CC and SS edge conditions. (*l/h*=0.5, *n*=1, *h/b*=0.1).

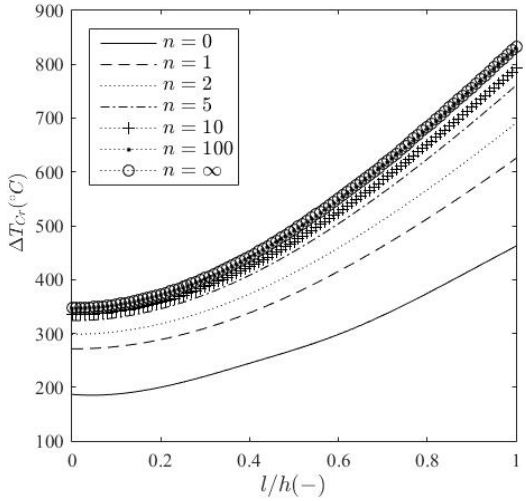

Fig.5
Influence of the volume fraction index *n* on the variation of ΔT_{cr} with *l/h* of nano plate without foundation, for case TD with CC edge conditions (β=0.5*, h/b*=0.1).

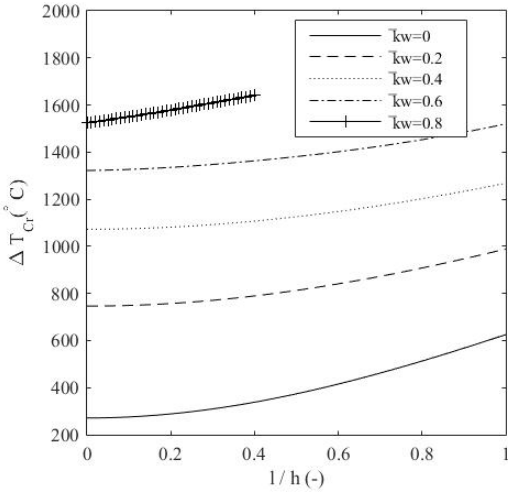

Fig.6
Influence of dimensionless Winkler stiffness coefficient $\bar{k}_w$ on the variation of ΔT_{cr} with *l/h* of nano plate with CC edge conditions and TD case (*n*=1 , β=0.5*,, h/b*=0.1*; k_s*=0.0).

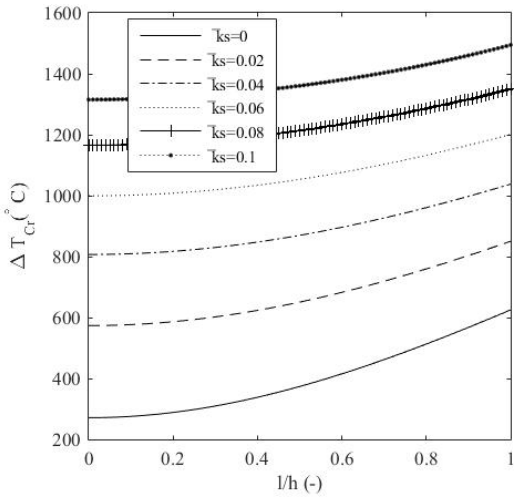

Fig.7

Influence of dimensionless Pasternak stiffness coefficient $\overline{k}_s$ on the variation of ΔT_{cr} with *l/h* of nano plate with CC edge conditions and TD case (n=1 , β=0.5,, h/b=0.1; kw=0.0).

ACKNOWLEDGMENT

Not applicable.

REFERENCES

[1] Fleck, N.A., and Hutchinson, J.W., 1993, A Phenomenological Theory for Strain Gradient Effects in Plasticity, Journal of Mechanics and Physics of Solids, 41(12): 1825–57.

[2] Yang, F., Chong, A.C.M. , Lam, D.C.C., 2002, Tong, P., Couple Stress Based Strain Gradient Theory for Elasticity, International Journal of Solids and Structures, 39: 2731–43

[3] Duan W.H., Wang C.M., 2009, Nonlinear bending and stretching of a circular graphene sheet under a central point load, Nanotechnology, 20: 1-7.

[4] Shen L., Shen H.S. Zhang C.L., 2010, Nonlocal plate model for nonlinear vibration of single layer graphene sheets in thermal environments, Computational Materials Science, 48: 680–685.

[5] Jabbarzadeh, M., Talati, H., Noroozi, A.R., 2013, Nonlinear Analysis of Circular Graphene Sheet Using Nonlocal Continuum Mechanic Theory, Journal of Modares Mechanical Engineering, 13(13): 57-66 (In Persian).

[6] Wang, Y.G., Lin, W.H., Liu, N., 2013, Large Amplitude Free Vibration of Size-Dependent Circular Microplates Based on the Modified Couple Stress Theory, International Journal of Mechanical Science., 71: 51-57.

[7] Ghiasian, S.E., Kiani, Y., Sadighi, M., Eslami, M.R., 2014. Thermal Buckling of Shear Deformable Temperature Dependent Circular/Annular FGM Plates, International Journal of Mechanical Science, 81: 137-148.

[8] Jabbari, M., Hashemitaheri, M, Mojahedin, A, 2014, Thermal Buckling Analysis of Functionally Graded Thin Circular Plate Made of Saturated Porous Materials, Journal of Thermal Stress, 3: 202–220.

[9] Ansari R., Gholami R, Faghih Shojaei M., Mohammadi V., Sahmani S., 2015, Bending, buckling and free vibration analysis of size-dependent functionally graded circular/annular microplates based on the modified strain gradient elasticity theory, European Journal of Mechanics A/Solids, 49: 251-267.

[10] Eshraghi, I., Dag, S., Soltani, N., 2016, Bending and Free Vibrations of Functionally Graded Annular and Circular Micro-Plates under Thermal Loading, Composite Structure, 137: 196-207.

[11] Shojaeefard M.H., Saeidi Googarchin, H, Ghadiri M., Mahinzare, M., 2017, Micro temperature-dependent FG porous plate: Free vibration and thermal buckling analysis using modifed couple stress theory with CPT and FSDT, Applied Mathematical Modeling, 50: 633-655.

[12] Lin, M.X., Lai, H.Y., Chen, C.K., 2017, Analysis of Nonlocal Nonlinear Behavior of Graphene Sheet Circular Nanoplate Actuators Subject to Uniform Hydrostatic Pressure, Microsystem Technology, 24: 919–928.

[13] Farzam, A., and Hassani, B., 2019, Size-Dependent Analysis of FG Microplates with Temperature-Dependent Material Properties Using Modified Strain Gradient Theory and Isogeometric Approach, Composites Part B, 161: 150-168.

[14] Gobadi. A, Tadi Beni, Y., Golestanian, H., 2020 , Size Dependent Nonlinear Bending Analysis of a Flexoelectric Functionally Graded Nano-Plate Under Thermo-Electro-Mechanical Loads, Journal of Solid Mechanics, 12(1) : 33-56.

[15] Ahmadpour, M., Golmakani, M.E., Malikan, M., 2021,Thermal Buckling Analysis of Circular Bilayer Graphene Sheets Resting on An Elastic Matrix Based on Nonlocal Continuum Mechanics, Journal of Applied Computational Mechanics, 7(4): 1862-1877.

[16] Rajabi M., Lexian , Rajabi A, 2021, Analysis of Nanoplate with a Central Crack Under Distributed Transverse Load Based on Modified Nonlocal Elasticity Theory, Journal of Solid Mechanics, 13(2): 213-232.

[17] Kiarasi F., Babaei M., Kamran Asemi K., Dimitri R., Tornabene F., 2021, Three-Dimensional Buckling Analysis of Functionally Graded Saturated Porous Rectangular Plates under Combined Loading Conditions, Applied Sciences, 11(21): 1-21.

[18] Saini R., Ahlawat N., Rai P., Khadimallah M.A., 2022, Thermal stability analysis of functionally graded non-uniform asymmetric circular and annular nano discs: Size-dependent regularity and boundary conditions, Europian Journal of Mechanics-A/Solids, 94:51-65.

[19] Jalali, S.K., and Heshmati, M.,2020, Vibration Analysis of Tapered Circular Poroelastic Plates with Radially Graded Porosity Using Pseudo-Spectral Method, Mechanics of Materials, 140.

[20] Jalali, S.K., Naei, M.H., Poorsolhjouy, A., 2010, Thermal Stability Analysis of Circular Functionally Graded Sandwich Plates of Variable Thickness Using Pseudo-Spectral Method, Materials and Design, 31: 4755-4763.

[21] Brush, D.O, and Almroth, B.O., 1975,Buckling of Bars Plates and Shells, McGraw-Hill, New York, Second Edition.